atoms

MDPI

Article

Interaction of Be^{4+} and Ground State Hydrogen Atom—Classical Treatment of the Collision

I. Ziaeian and K. Tőkési *

Institute for Nuclear Research, ATOMKI, Debrecen, Hungary; iman.zia@atomki.mta.hu
* Correspondence: tokesi@atomki.mta.hu

Received: 30 March 2020; Accepted: 28 May 2020; Published: 3 June 2020

Abstract: The interaction between Be^{4+} and hydrogen atom is studied using the three-body classical trajectory Monte Carlo method (CTMC) and quasiclassical trajectory Monte Carlo method of Kirschbaum and Wilets (QTMC-KW). We present total cross sections for target ionization, target excitation, and charge exchange to the projectile bound state. Calculations are carried out in the projectile energy range between 10 and 1000 keV/au, relevant to the interest of fusion research when the target hydrogen atom is in the ground state. Our results are compared with previous theoretical results. We found that the classical treatment describes reasonably well the cross sections for various final channels. Moreover, we show that the calculations by the QTMC-KW model significantly improve the obtained cross sections.

Keywords: classical trajectory Monte Carlo method; ionization; excitation; charge exchange

1. Introduction

The currently used energy production methods will not be able to satisfy the energy needs of humanity in the long run. One of the best solutions in the future would be the implementation of fusion power plants. Beryllium is typically considered as the armor material for plasma facing components (PFCs) of fusion devices and it is the first wall of the international thermonuclear experimental reactor (ITER) [1]. Chemical and physical erosion of the first wall releases beryllium atoms and several molecular species, which eventually lead to the presence of fully-stripped beryllium ions in the plasma core. Beryllium is attractive as a plasma facing reactor material because of its low atomic number (i.e., low potential for radiative plasma power losses), excellent gettering properties concerning oxygen (unavoidably present in any fusion plasma), and adequate thermo-mechanical and erosion properties when exposed to plasma energy and particle fluxes. The inelastic collision processes between Be^{q+} ions and H are particularly important when energetic neutral hydrogen is injected into the plasma for heating and diagnostic purposes [2]. Therefore, the accurate description and knowledge of these interactions are extremely important for fusion research.

The calculation of cross section in collision Be^{4+} and hydrogen atom for ionization, charge exchange and excitation channels were studied using different theoretical approaches such as:

i. Atomic-orbital close-coupling (AOCC) [3,4]
ii. Adiabatic superpromotion model [5]
iii. The molecular orbital expansion of the solution of the time-dependent Schrodinger equation [6]
iv. Symmetric Eikonal approximation [7]
v. Classical methods [8]

In the last two decades, there has been a great revival of the classical trajectory Monte Carlo (CTMC) calculations applied in atomic collisions involving three or more particles. This approximation

is useful in treating atomic collisions where the quantum mechanical ones become very complicated or unfeasible [8]. One of the advantages of the CTMC method is that many-body interactions are exactly taken into account during the collisions on a classical level. The CTMC method is a non-perturbative method, where classical equations of motions are solved numerically [9–11]. The quasiclassical trajectory Monte Carlo method of Kirschbaum and Wilets (QTMC-KW) model represents one step further towards a better description of the classical atomic collisions. In particular, it is desirable to have a method that consistently treats electron transfer and ionization as well as multiplicities and combinations of these processes. For atoms, a necessary condition for stability is that the electrons are not allowed to collapse to the symmetry point, i.e., to the nucleus. The effective potential enforcing this condition is motivated by the Heisenberg uncertainty principle $rp \geq \xi_H \hbar$, where r and p are the distance and momentum of an electron with respect to a nucleus and ξ_H is constant. For the H atom, this condition is equivalent to the de Broglie description of the hydrogen atom. Also, a classical Pauli constraint means that any two electrons having the same spins cannot occupy the same volume of phase space. We effect this by requiring that $r_{ij} p_{ij} \geq \xi_P$, where $\vec{r}_{ij}$, is the relative position and $\vec{p}_{ij}$, is the relative momentum of the ith and jth identical electrons, and ξ_P is another dimensionless constant which must be determined.

The QTMC-KW [12] has now been applied to a variety of different problems [13]. The method and its extensions [14–18] use momentum-dependent effective potentials in a Hamiltonian model to stabilize realistic atomic and molecular structures, which would otherwise autoionize classically. In this work, the interaction between Be^{4+} and ground state hydrogen atom is studied using the three-body CTMC and QTMC-KW in the projectile energy range between 10 and 1000 keV/au.

2. Theory

2.1. CTMC Method

In the present work, the CTMC simulations were made in the three-body approximation. The three particles (p; projectile, e; electron, T; target) are characterized by their masses and charges. For the description of the interaction among the particles, Coulomb potential is used. Figure 1 shows the relative position vectors of the three-body collision system.

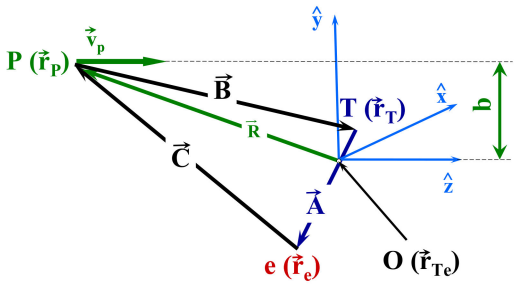

Figure 1. The relative position vectors of the particles involved in 3-body collisions. $\vec{A} = \vec{r}_e - \vec{r}_T$, $\vec{B} = \vec{r}_T - \vec{r}_p$ and $\vec{C} = \vec{r}_p - \vec{r}_e$, in such way that $\vec{A} + \vec{B} + \vec{C} = 0$. Also, $\vec{r}_{Te}$ is the position vector of the center-of-mass of the target system, and b is the impact parameter.

The Hamiltonian equation for the three particles can be written as:

$$H_0 = T + V_{coul} \tag{1}$$

where

$$T = \frac{\vec{P}_p^2}{2m_p} + \frac{\vec{P}_e^2}{2m_e} + \frac{\vec{P}_T^2}{2m_T} \tag{2}$$

and

$$V_{coul} = \frac{Z_p Z_e}{\left|\vec{r}_p - \vec{r}_e\right|} + \frac{Z_e Z_T}{\left|\vec{r}_e - \vec{r}_T\right|} + \frac{Z_p Z_T}{\left|\vec{r}_p - \vec{r}_T\right|} \tag{3}$$

where T and V_{coul} are total kinetic energy and the potential energy term. $\vec{r}$, $\vec{p}$, Z, and m are the position vector, momentum vector, the charge and the mass of the corresponding particles, respectively. The equations of motion taking into account the Hamiltonian mechanics is given as follows:

$$\dot{\vec{P}}_e = -\frac{\delta H}{\delta \vec{r}_e} = -\frac{Z_p Z_e}{\left|\vec{r}_p - \vec{r}_e\right|^3}\left(\vec{r}_p - \vec{r}_e\right) + \frac{Z_e Z_T}{\left|\vec{r}_e - \vec{r}_T\right|^3}\left(\vec{r}_e - \vec{r}_T\right) \tag{4}$$

$$\dot{\vec{P}}_T = -\frac{\delta H}{\delta \vec{r}_T} = -\frac{Z_p Z_T}{\left|\vec{r}_p - \vec{r}_T\right|^3}\left(\vec{r}_p - \vec{r}_T\right) - \frac{Z_e Z_T}{\left|\vec{r}_e - \vec{r}_T\right|^3}\left(\vec{r}_e - \vec{r}_T\right) \tag{5}$$

$$\dot{\vec{P}}_p = -\frac{\delta H_{FMD}}{\delta \vec{r}_p} = \frac{Z_p Z_e}{\left|\vec{r}_p - \vec{r}_e\right|^3}\left(\vec{r}_p - \vec{r}_e\right) + \frac{Z_p Z_T}{\left|\vec{r}_p - \vec{r}_T\right|^3}\left(\vec{r}_p - \vec{r}_T\right) \tag{6}$$

Introducing the relative position vectors $\vec{A} = \vec{r}_e - \vec{r}_T$, $\vec{B} = \vec{r}_T - \vec{r}_p$ and $\vec{C} = \vec{r}_p - \vec{r}_e$, in such a way that $\vec{A} + \vec{B} + \vec{C} = \vec{0}$ as well as the definition of $N = \frac{1}{m}$, the Equations (4)–(6) are reduced to the following:

$$\ddot{\vec{A}} = \left\{\frac{N_e Z_p Z_e}{\left|\vec{A} + \vec{B}\right|^3} + \frac{(N_e + N_T) Z_e Z_T}{\left|\vec{A}\right|^3}\right\}\vec{A} + \left\{\frac{N_e Z_p Z_e}{\left|\vec{A} + \vec{B}\right|^3} - \frac{N_T Z_p Z_T}{\left|\vec{B}\right|^3}\right\}\vec{B} \tag{7}$$

$$\ddot{\vec{B}} = \left\{\frac{N_p Z_p Z_e}{\left|\vec{A} + \vec{B}\right|^3} - \frac{N_T Z_e Z_T}{\left|\vec{A}\right|^3}\right\}\vec{A} + \left\{\frac{\left(N_T + N_p\right) Z_p Z_T}{\left|\vec{B}\right|^3} + \frac{N_p Z_p Z_e}{\left|\vec{A} + \vec{B}\right|^3}\right\}\vec{B} \tag{8}$$

The initial conditions of the collisions system, i.e., the coordinates and the velocities of an internal motion of (T,e) atomic system and the relative projectile and atomic center-of-mass motion were selected randomly. Equations (7) and (8) were integrated with respect to the time as an independent variable by the standard Runge–Kutta method for a given set of initial conditions as described by Tőkési and Kövér [19].

The total cross-sections were computed with the following formulas:

$$\sigma = \frac{2\pi b_{max}}{T_N} \sum_j b_j^{(i)} \tag{9}$$

The statistical uncertainty of the cross section is given by:

$$\Delta\sigma = \sigma\left(\frac{T_N - T_N^{(i)}}{T_N T_N^{(i)}}\right)^{\frac{1}{2}} \tag{10}$$

where T_N is the total number of trajectories calculated for impact parameters less than b_{max}, $T_N^{(i)}$ is the number of trajectories that satisfy the criteria for the corresponding final channels (ionization, excitation, charge exchange) and $b_j^{(i)}$ is the actual impact parameter for the trajectory corresponding to ionization, excitation or charge exchange processes.

In the CTMC calculations, the energy level E of an electron after the excitation is determined simply by calculating its binding energy $U = -E$. A classical principal quantum number is assigned according to:

$$n_c = Z_T Z_e \left(\frac{\mu_{Te}}{2U}\right)^{1/2} \tag{11}$$

where μ_{Te} is the reduced mass between the target nucleus and the target electron. The classical values of nc are "quantized" to a specific level n [20] if they satisfy the relation:

$$[(n-1)(n-1/2)n]^{1/3} \leq n_c \leq [(n+1)(n+1/2)n]^{1/3} \tag{12}$$

The classical orbital angular momentum is defined by

$$l_c = \sqrt{m_e\left[\left(x\dot{y} - y\dot{x}\right)^2 + \left(x\dot{z} - z\dot{x}\right)^2 + \left(y\dot{z} - z\dot{y}\right)^2\right]}, \tag{13}$$

where x, y, and z are the Cartesian coordinates of the electron relative to the nucleus. Since lc is uniformly distributed for a given n level [21], the quantal statistical weights are reproduced by choosing bin sizes such that

$$l \leq \frac{n}{n_c} l_c \leq l + 1, \tag{14}$$

where l is the quantum-mechanical orbital-angular-momentum. The choice of bins in classical microcanonical ensemble n_C and l_C by a principle of proportionality of classical and quantal weights is discussed in detail by Becker and Mackellar [20].

2.2. QTMC-KW Method

For the more accurate classical simulation results, we must also consider the rule of Heisenberg and Pauli principles. This approach was proposed by Kirschbaum and Wilets (KW) [12] in the dominant of the fermion molecular dynamic model (FMD). They added effective potentials, V_H and V_P, motivated by the Heisenberg and Pauli principles, to the pure Coulomb inter-particle potentials describing the atom. Thus,

$$H_{FMD} = H_0 + V_H + V_P \tag{15}$$

where H_0 is the usual Hamiltonian containing the total kinetic energy of all bodies and Coulomb potential terms between all pairs of electrons and between the nucleus and electrons, respectively. The extra terms are

$$V_H = \sum_{n=a,b} \sum_{i=1}^{N} f(r_{ni}\ , p_{ni}; \xi_H\ ,\ \alpha_H) \tag{16}$$

and

$$V_p = \sum_{i=1}^{N} \sum_{j=i+1}^{N} f\left(r_{ij}\ , p_{ij}; \xi_p\ ,\ \alpha_p\right)\delta_{s_i,s_j} \tag{17}$$

where a and b denote the nuclei, while i and j index the electrons. Also, $r_{\alpha\beta} = r_\beta - r_\alpha$ and relative momenta are:

$$p_{\alpha\beta} = \frac{m_\alpha p_\beta - m_\beta m_\alpha}{m_\alpha + m_\beta} \tag{18}$$

and $\delta_{s_i,s_j} = 1$ if the spins of the ith and jth electrons are the same and 0 if they are different. The constraining potentials are chosen of the form

$$f(r_{\lambda\nu}\ , p_{\lambda\nu}; \xi\ ,\ \alpha) = \frac{\xi}{4\alpha r_{\lambda\nu}^2 \mu_{\lambda\nu}} exp\left\{\alpha\left[1 - \left(\frac{r_{\lambda\nu} p_{\lambda\nu}}{\xi}\right)^4\right]\right\} \tag{19}$$

In this work, in the case of hydrogen as a one electron target we just take into account the Heisenberg constrain and the parameters universally used where $\alpha_H = 4$ and $\xi_H = 0.9428$, respectively and we used these parameters in our calculations as well. Also, the Heisenberg potential should be considered between electron and both target and projectile nucleus as follows:

$$f\left(\vec{r}_{pe}\,,\vec{P}_{pe};\varepsilon_H\,,\,\alpha_H\right)=\frac{{\xi_H}^2}{4\alpha_H\,\vec{r}^{\,2}_{pe}\mu_{pe}}exp\left\{\alpha_H\left[1-\left(\frac{\vec{r}_{pe}\vec{P}_{pe}}{\xi_H}\right)^4\right]\right\} \tag{20}$$

$$f\left(\vec{r}_{Te}\,,\vec{P}_{Te};\varepsilon_H\,,\,\alpha_H\right)=\frac{{\xi_H}^2}{4\alpha_H\,\vec{r}^{\,2}_{Te}\mu_{Te}}exp\left\{\alpha_H\left[1-\left(\frac{\vec{r}_{Te}\vec{P}_{Te}}{\xi_H}\right)^4\right]\right\} \tag{21}$$

According to Figure 1, the equations of motion taking into account the Hamiltonian mechanics besides the extra potential is given by:

$$\begin{aligned}\ddot{\vec{A}}=&\left[\frac{N_eZ_pZ_e}{\left|\vec{A}+\vec{B}\right|^3}+\frac{(N_e+N_T)Z_eZ_T}{\left|\vec{A}\right|^3}+\frac{{\xi_H}^2(N_e+N_T)^2}{2\alpha_H\left|\vec{A}\right|^4}e^{\alpha_H[1-(\frac{|\vec{A}\|\vec{P}_{Te}|}{\xi_H})^4]}\right.\\&+\frac{\vec{P}^4_{Te}(N_T+N_e)^2}{{\xi_H}^2}e^{\alpha_H[1-(\frac{|\vec{A}\|\vec{P}_{Te}|}{\xi_H})^4]}\\&+\frac{{\xi_H}^2N_e\left(N_e+N_p\right)}{2\alpha_H\left|\vec{A}+\vec{B}\right|^4}e^{\alpha_H[1-(\frac{|\vec{A}+\vec{B}\|\vec{P}_{ep}|}{\xi_H})^4]}\\&\left.+\frac{\vec{P}^4_{ep}N_e\left(N_e+N_p\right)}{{\xi_H}^2}e^{\alpha_H[1-(\frac{|\vec{A}+\vec{B}\|\vec{P}_{ep}|}{\xi_H})^4]}\right]\vec{A}\\&+\left[\frac{N_eZ_pZ_e}{\left|\vec{A}+\vec{B}\right|^3}-\frac{N_TZ_pZ_T}{\left|\vec{B}\right|^3}+\frac{{\xi_H}^2N_e\left(N_e+N_p\right)}{2\alpha_H\left|\vec{A}+\vec{B}\right|^4}e^{\alpha_H[1-(\frac{|\vec{A}+\vec{B}\|\vec{P}_{ep}|}{\xi_H})^4]}\right.\\&\left.+\frac{\vec{P}^4_{ep}N_e\left(N_e+N_p\right)}{{\xi_H}^2}e^{\alpha_H[1-(\frac{|\vec{A}+\vec{B}\|\vec{P}_{ep}|}{\xi_H})^4]}\right]\vec{B}\end{aligned} \tag{22}$$

$$\begin{aligned}\ddot{\vec{B}}=&\left[\frac{N_pZ_pZ_e}{\left|\vec{A}+\vec{B}\right|^3}-\frac{N_TZ_eZ_T}{\left|\vec{A}\right|^3}-\frac{{\xi_H}^2N_T(N_e+N_T)}{2\alpha_H\left|\vec{A}\right|^4}e^{\alpha_H[1-(\frac{|\vec{A}\|\vec{P}_{Te}|}{\xi_H})^4]}\right.\\&-\frac{\vec{P}^4_{Te}N_T(N_e+N_T)}{{\xi_H}^2}e^{\alpha_H[1-(\frac{|\vec{A}\|\vec{P}_{Te}|}{\xi_H})^4]}\\&+\frac{{\xi_H}^2N_p\left(N_e+N_p\right)}{2\alpha_H\left|\vec{A}+\vec{B}\right|^4}e^{\alpha_H[1-(\frac{|\vec{A}+\vec{B}\|\vec{P}_{ep}|}{\xi_H})^4]}\\&\left.+\frac{\vec{P}^4_{ep}N_p\left(N_e+N_p\right)}{{\xi_H}^2}e^{\alpha_H[1-(\frac{|\vec{A}+\vec{B}\|\vec{P}_{ep}|}{\xi_H})^4]}\right]\vec{A}\\&+\left[\frac{\left(N_T+N_p\right)Z_pZ_T}{\left|\vec{B}\right|^3}+\frac{N_pZ_pZ_e}{\left|\vec{A}+\vec{B}\right|^3}+\frac{{\xi_H}^2N_p\left(N_e+N_p\right)}{2\alpha_H\left|\vec{A}+\vec{B}\right|^4}e^{\alpha_H[1-(\frac{|\vec{A}+\vec{B}\|\vec{P}_{ep}|}{\xi_H})^4]}\right.\\&\left.+\frac{\vec{P}^4_{ep}N_p\left(N_e+N_p\right)}{{\xi_H}^2}e^{\alpha_H[1-(\frac{|\vec{A}+\vec{B}\|\vec{P}_{ep}|}{\xi_H})^4]}\right]\vec{B}\end{aligned} \tag{23}$$

3. Results and Discussion

To study the collision between Be^{4+} and hydrogen atoms, we used both the standard three-body classical trajectory Monte Carlo (CTMC) and quasiclassical trajectory Monte Carlo method of Kirschbaum and Wilets (QTMC-KW) methods. We performed a classical simulation with an ensemble of $1{\times}10^6$ primary trajectories for each energy. The calculations are carried out in the projectile energy range between 10 and 1000 keV/au, relevant to the interest of the fusion research when the target hydrogen atom is in the ground state. We estimate uncertainties in our calculation 0.6% error. This error has been obtained by the standard statistical error in σ (see Equation (10)). Furthermore, we note that, according to our knowledge, this is the first time to present cross section data using the QTMC-KW method for the Be^{4+} + H(1s) system.

3.1. Ionization

For the illustration of the ionization channel, defined by Equation (24), Figure 2 shows typical trajectories in the y–z coordinate system (a) and y position as a function of time (b) for three bodies (projectile, electron, and target) in the lab frame, respectively. The trajectories were obtained at 900 keV/au projectile impact.

$$Be^{4+} + H(1s) \rightarrow Be^{4+} + H^+ + e^- \quad (24)$$

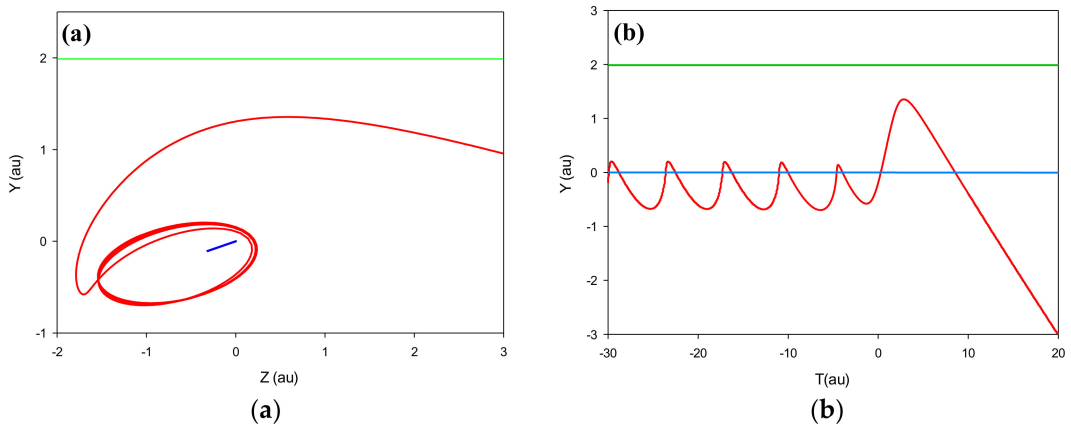

Figure 2. (**a**) Trajectories in the y-z lab frame, (**b**) y position as a function of time for the electron (red line), projectile (green line) and target (blue line) for ionization channel for a typical Be^{4+} with E = 900 keV/au.

Figure 3 shows the ionization cross section obtained by both the CTMC and QTMC-KW methods as a function of projectile energy in the energy range between 10 and 1000 keV/au. The results of the present CTMC models are compared with the previous results. Our results with CTMC method match the data of Olson [9] for the entire energy range. At the same time, our results show lower cross section data than that obtained by Krstic and Radmilovic [5] for lower projectile energies. Applying the effective potentials, V_H, to mimic the Heisenberg principles in our simulations, the cross section data are a little increased compared to the standard CTMC results.

3.2. Charge Exchange (CX)

The accurate knowledge of the charge exchange cross sections in fusion plasma is very important. For example, the charge exchange recombination spectroscopy (CXRS) measurements using Be^{4+} provide a high-quality determination of the plasma parameters. The quality of such concentration measurements relies on the accuracy of the charge exchange cross sections.

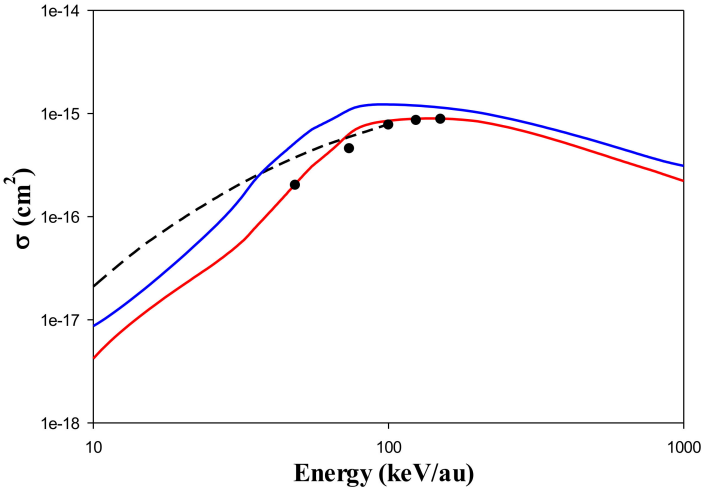

Figure 3. Cross section for ionization of H(1s) by Be^{4+} as a function of projectile energy. CTMC (red solid line), QTMC-KW (blue solid line), Reference [5] (dash line), Reference [9] (•).

Figure 4 represents typical classical trajectories for the charge exchange channel. The trajectory calculations were performed at 900 keV/au impact energy. Furthermore, we have calculated the total cross section of CX to the projectile bound state according to CTMC and QTMC-KW methods for the process:

$$Be^{4+} + H(1s) \rightarrow Be^{3+}(nl) + H^{+} \quad (25)$$

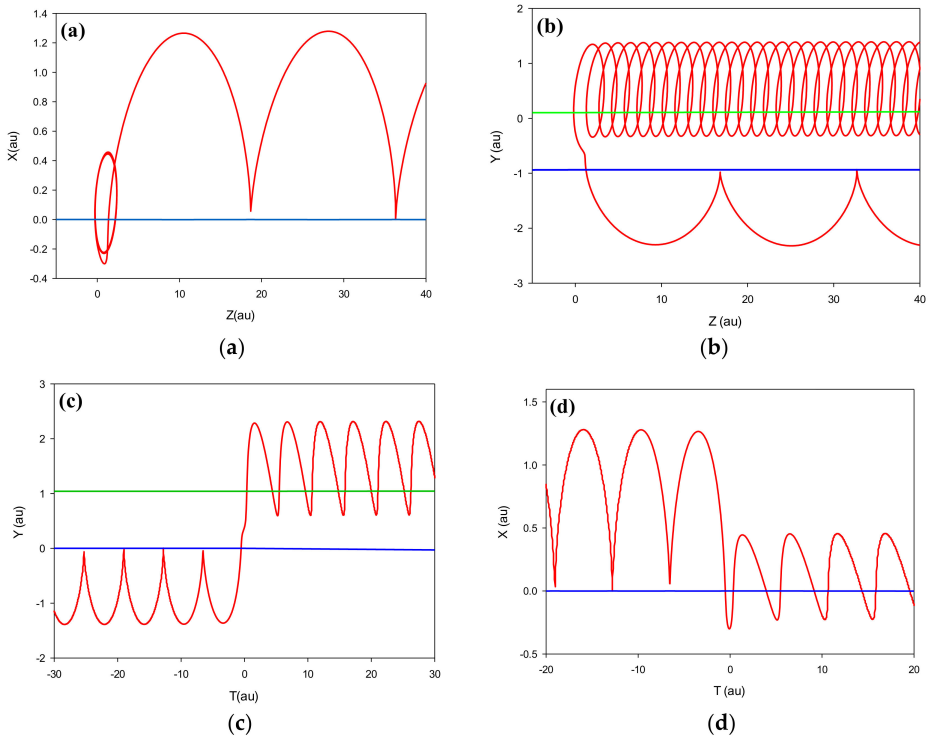

Figure 4. (**a**) Trajectories in the *x*-*z* projectile frame, (**b**) Trajectories in the *y*-*z* center-of-mass frame, (**c**) *y* position as a function of time in the lab frame, (**d**) *x* position as a function of time in the projectile frame for the electron (red line), projectile (green line) and target (blue line) for charge exchange channel for a typical Be^{4+} with E = 900 keV/au.

The comparisons were made with all available methods such as the solution of time-dependent Schroedinger equations, molecular-orbital-close coupling (MOCC), and atomic-orbital-close coupling (AOCC) calculations (see Figure 5).

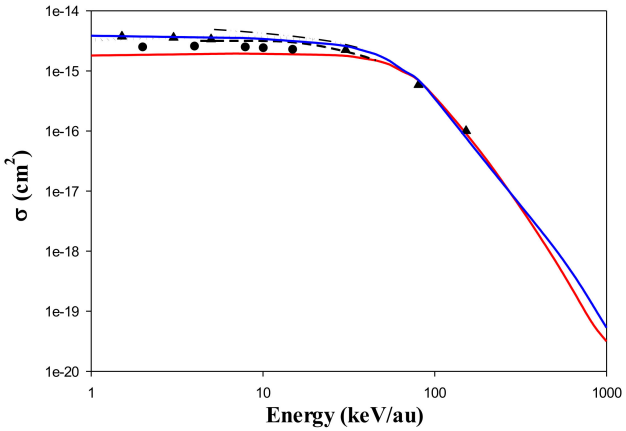

Figure 5. Total cross section for charge exchange in Be^{4+} + H(1s) collision, as a function of the impact energy. CTMC (solid red line), QTMC-KW (solid blue line), Reference [22] (dash line), Reference [23] (-..-..), Reference [24] (. . .), Reference [6] (•), Reference [4] (▲).

We found a significant improvement in the cross section using the QTMC-KW method compared to the standard CTMC model. We also found excellent agreement between our QTMC-KW results and the previous data by Qu et al. [4], Ludde et al. [22], Bransden et al. [23], and Harel et al. [24].

3.3. Excitation

In the following, we show cross sections for Be^{4+} induced $1s \rightarrow 2s$ and $1s \rightarrow 2p$ transitions in atomic hydrogen by using CTMC and QTMC-KW methods. The excitation process is given as follows:

$$Be^{4+} + H(1s) \rightarrow Be^{4+} + H(n,l,m)^{*} \tag{26}$$

We considered the excitation of hydrogen atom by beryllium from 1s state to 2s and 2p excited states. Hence, the hydrogen's electron transmits to quantum numbers $n = 2$ and $l = 0,1$ which correspond to spherical (s) or polar (p) orbital-angular-momentum, respectively.

Figure 6a,b represent the y position as a function of time and 3D trajectory in the lab frame in CTMC method for three bodies (projectile, electron and target), respectively. These figures have been established for a typical projectile with the energy of 900 keV/au.

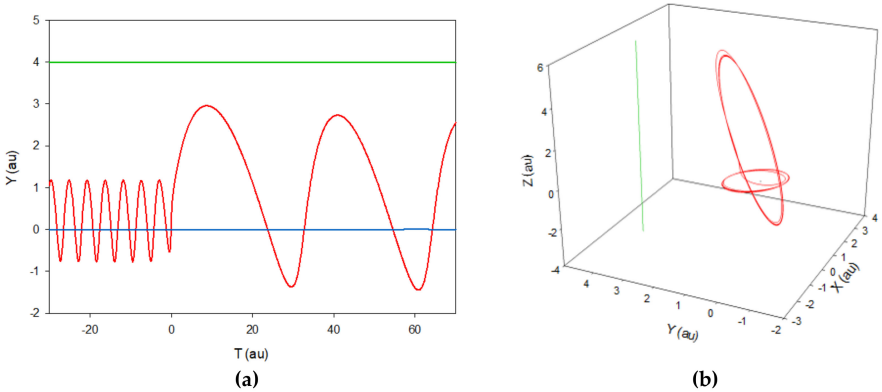

Figure 6. (**a**) y position trajectory as a function of time in the lab frame, (**b**) 3D Trajectory in the lab frame for the electron (red line), projectile (green line) and target (blue line) for excitation channel for a typical Be^{4+} with E = 900 keV/au.

Figure 7 shows the excitation cross section in Be^{+4} + H(1s) collisions as a function of projectile energy for $H(1s) \rightarrow H(2s)$ (see Figure 7a) and $H(1s) \rightarrow H(2p)$ (see Figure 7b) transition states, respectively. The comparisons were made with the corresponding results based on adiabatic superpromotion model [5], symmetric Eikonal approximation [7] as well as AOCC calculations [25].

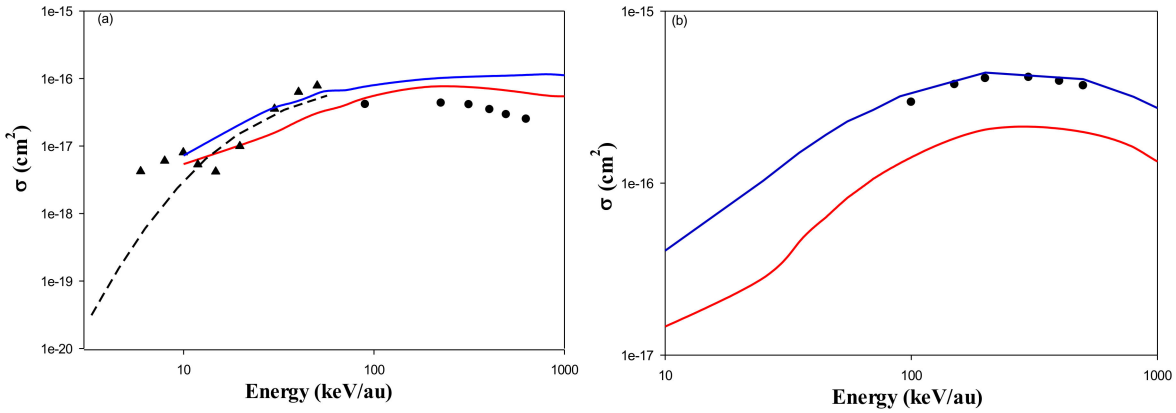

Figure 7. Cross section for the excitation of (**a**) $nl = 2s$ and (**b**) $nl = 2p$ hydrogen level in Be^{4+} + H(1s).collision, as a function of the impact energy. CTMC (solid red line), QTMC-KW (solid blue line), Reference [5] (dash line), Reference [25] (▲), Reference [7] (•).

We note that, while in the previous works, the obtained excitation cross sections are from H(1s) to H(n = 2), in our work, we show cross sections into H(2s) and H(2p) subshells. As shown in Figure 7, both CTMC and QTMC-KW methods are useful to describe the excitation cross section for H(1s) to H(2s) transition state. Furthermore, using QTMC-KW model one can see that the cross sections data are shifted to higher values compared to the CTMC data. It is noticeable that the data obtained by the QTMC-KW model are in good agreement with the data reported by the symmetric Eikonal approximation results [7].

4. Conclusions

Cross sections for ionization, charge exchange, and low-level excitation channels were simulated for a Be^{4+}+H(1s) collision system using the classical trajectory Monte Carlo method (CTMC) and quasiclassical trajectory Monte Carlo method of Kirschbaum and Wilets (QTMC-KW). To increase of calculation's accuracy, we considered one million trajectories for each impact parameter. Also, we estimate uncertainties in our 0.6% calculation error.

We draw the conclusion that the classical treatment can describe the calculated cross sections reasonably. While there is no experimental data for the mentioned collision system, we compared our results with the previous literature based on other methods, such as AOCC, MOCC, adiabatic superpromotion model, and Symmetric Eikonal approximation. We found that our calculations are in good agreement with previous results.

Author Contributions: I.Z. and K.T. discussed the results and contributed to the final manuscript. I.Z.: development of CTMC code, performance of analytical and numerical calculations. K.T.: development of CTMC code, performance of analytical calculations and supervised the project. All authors have read and agreed to the published version of the manuscript.

Funding: The work was support by the National Research, Development and Innovation Office (NKFIH) Grant KH126886.

Acknowledgments: The work was support by the National Research, Development and Innovation Office (NKFIH) Grant KH126886. This work has been carried out within the framework of the EURO fusion Consortium and has received funding from the Euratom research and training program 2014-2018 under grant agreement No 633053. The views and opinions expressed herein do not necessarily react to those of the European Commission.

Conflicts of Interest: The authors declare no conflict of interest.

References

1. Pitts, R.; Carpentier, S.; Escourbiac, F.; Hirai, T.; Komarov, V.; Kukushkin, A.; Lisgo, S.; Loarte, A.; Merola, M.; Mitteau, R.; et al. Physics basis and design of the ITER plasma-facing components. *J. Nucl. Mater.* **2011**, *415*, S957–S964. [CrossRef]
2. Hackman, J.; Uhlenbusch, J. Test of a beryllium limiter in the tokamak unitor. *J. Nucl. Mater.* **1984**, *128/129*, 418–421. [CrossRef]
3. Igenbergs, K.; Schweinzer, J.; Aumayer, F. Charge exchange in Be^{4+} -H(n=1,2) collision studied systematically by atomic-orbital close-coupling calculations. *J. Phys. B: At. Mol. Opt. Phys.* **2009**, *42*, 1–8. [CrossRef]
4. Qu, Y.Z.; Liu, L.; Liu, C.H.; Li, T.C.; Wang, J.G.; Janev, R.K. Charge transfer cross section calculation and evaluation for Be^{q+} + H collisions. In Proceedings of the Eighth International Conference on Atomic and Molecular Data and Their Applications, NIST, Cambridge, MA, USA, 30 September –4 October 2012; pp. 232–241.
5. Krstic, P.S.; Radmilovic, M. Charge exchange, excitation and ionization in slow Be^{4+} + H and B^{5+} + H collisions. *J. Nuclear Fusion.* **1992**, *3*, 113–125.
6. Kimura, M.; Thorson, W.R. Molecular-state studies of charge transfer in Li^{3+}-H, Be^{4+}-H and B^{5+}-H collisions. *J. Phys. B At. Mol. Phys.* **1983**, *16*, 1471–1480. [CrossRef]
7. Olivera, G.H.; Ramirez, C.A.; Rivarola, R.D. Cross-Sections for Excitation and Ionization of Helium and Hydrogen by Be4+ and B6+ Ions. *Physica Scripta.* **1996**, *T62*, 84–87. [CrossRef]
8. Olson, R.E.; Reinhold, C.O.; Schultz, D.R. High-Energy Ion-Atom Collisions. In Proceedings of the IVth Workshop on High-Energy Ion-Atom Collision Processes, Debrecen, Hungary, 17–19 September 1990.
9. Olson, R.E.; Salop, A. Charge-transfer and impact-ionization cross sections for fully and partially stripped positive ions colliding with atomic hydrogen. *Phys. Rev. A* **1977**, *16*, 531–541. [CrossRef]
10. Tőkési, K.; Hock, G. Versatility of the exit channels in the three-body CTMC method. *Nucl. Instrum Meth. Phys. Res. B* **1994**, *86*, 201–204. [CrossRef]
11. Tőkési, K.; Hock, G. Double electron capture in collision up to 1500 keV/amu projectile impac. *J. Phys. B* **1996**, *29*, L119–L125. [CrossRef]
12. Kirschbaun, C.L.; Wilet, L. Classical many-body model for atomic collisions incorporating the Heisenberg and Pauli principles. *Phys. Rev. A* **1980**, *21*, 834–841. [CrossRef]
13. Wilet, L.; Cohen, J.S. Fermion molecular dynamics in atomic, molecular and optical Physics. *Contemp. Phys.* **1998**, *39*, 163–175. [CrossRef]
14. Cohen, J.S. Molecular effects on antiproton capture by H_2 and the states of pp formed. *Phys. Rev. A.* **1997**, *56*, 3583–3596. [CrossRef]
15. Cohen, J.S. Extension of quasiclassical effective Hamiltonian structure of atoms through Z=94. *Phys. Rev. A* **1998**, *57*, 4964–4966. [CrossRef]
16. Cohen, J.S. Multielectron effects in capture of antiprotons and muons by helium and neon. *Phys. Rev. A* **2000**, *62*, 022512. [CrossRef]
17. Jorge, A.; Illescas, C.; Mendez, L.; Pons, B. Switching classical trajectory Monte Carlo method to describe two-active-electron collisions. *Phys. Rev. A* **2016**, *94*, 022710. [CrossRef]
18. Nicolas, B.; Otranto, S. Evaluation of differential cross sections using classical two-active electron models for He. *Eur. Phys. J. D.* **2019**, *73*, 1–6.
19. Tőkési, K.; Kövér, Á. Electron capture to the continuum at 54.4 eV positron-argon atom collisions. *J. Phys. B* **2000**, *33*, 3067–3077. [CrossRef]
20. Becker, R.L.; Mackellar, A. Theoretical initial *l* dependence of ion-Rydberg-atom collision cross sections. *J. Phys. B At. Mol. Opt. Phys.* **1984**, *17*, 3923–3942. [CrossRef]
21. Tőkési, K.; Mukoyama, T. Theoretical Investigation of ECC Peak for Charged Particles with the CTMC Method. *Bull Ins Chem Res Kyoto Univ.* **1994**, *72*, 62–68.
22. Ludde, H.J.; Dreizler, R.M. Electron capture with He^{2+}, Li^{3+}, Be^{4+} and B^{5+} projectiles from atomic hydrogen. *J. Phys. B At. Mol. Phys.* **1982**, *15*, 2713–2720. [CrossRef]
23. Bransden, B.H.; Newby, C.W.; Noble, C.J. Electron capture by fully stripped ions of helium, lithium, beryllium and boron from atomic hydrogen. *J. Phys. B At. Mol. Phys.* **1980**, *13*, 4245–4255. [CrossRef]

24. Harel, C.; Salin, A. Charge exchange in collision of highly ionised ions and atoms. *J. Phys. B At. Mol. Phys.* **1977**, *10*, 3511–3522. [CrossRef]
25. Fritsch, W.; Lin, C.D. Atomic-orbital-expansion studies of electron transfer in bare-nucleus Z (Z=2,4-8)-hydrogen-atom collision. *Phys. Rev. A* **1984**, *29*, 3039–3051. [CrossRef]